Inverse problem method for parameter estimation of a reaction-diffusion model of low grade gliomas

Amir Gholami, George Biros
Institute for Computational Engineering and Sciences, The University of Texas at Austin

The Question

If we are given two or more, partially observed, noisy serial scans of tumor, can we determine the full extend of tumor infiltration to healthy tissue and its spatio-temporal evolution?

Contributions

- Novel analytical and multi level Hessian preconditioners
- Fast, matrix-free Hessian-based algorithms
- A new Massively parallel, open source FFT solver for CPU and GPU (AccFFT library).

Problem Description

We seek to solve the following minimization problem:

$$\min_{p,k_f} \mathcal{J} := \frac{1}{2}\|Oc_0 - d_0\|^2_{L^2(\Omega)} + \frac{1}{2}\|Oc_1 - d_1\|^2_{L^2(\Omega)} + \frac{\beta_p}{2}\|p\|^2_{L^2(\Omega)} + \frac{\beta_k}{2}|k_f|^2, \quad (1)$$

subjected to:

$$\frac{\partial c}{\partial t} = \nabla \cdot (k\nabla c) + \rho c(1-c) \text{ in U with periodic B.Cs}, \quad (2)$$

$$c_0 = \Phi p \text{ in } \Omega, \quad (3)$$

where Ω is $[0, 2\pi]^3$, U is $\Omega \times (0, 1]$, c is the tumor concentration, O is the observation operator, d is the data, β is the regularization parameter, Φp is the tumor initial condition with Φ being a parametrization operator and p the corresponding parameters. Also, ρ is the tumor proliferation rate. The diffusion coefficient k is assumed to be inhomogeneous and anisotropic:

$$k = k_0(x) + k_f n(x) n(x)^T, \quad (4)$$

where $k_0(x)$ captures the inhomogeneity due to different diffusion rates in white/gray matter, $n(x)$ is the fiber structure directions derived from Diffusion Tensor Imaging, and k_f is a parameter adjusting the degree of anisotropic diffusion.

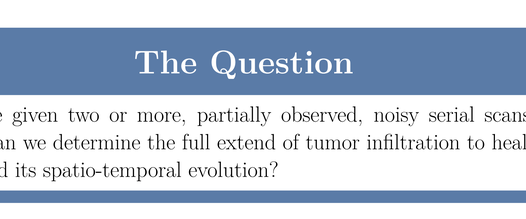

Figure 1: Left: An axial slice of the inhomogeneity in the tumor diffusion coefficient. Tumor cells diffuse faster in white matter areas compared to gray matter. Right: An exemplary fiber structure of the brain derived from diffusion tensor imaging data.

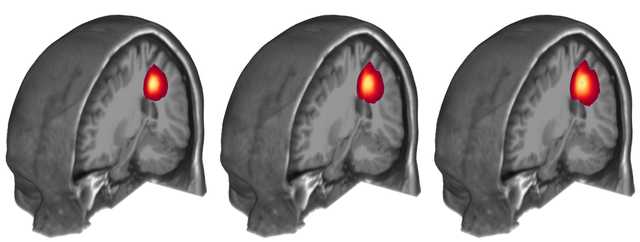

Figure 2: Forward simulation of tumor growth for a 28 month period, using the reaction-diffusion model of eq. (2).

Parallel Solver

The forward/adjoint equations are solved using Strang splitting, combined with pseudo-spectral method. The domain is distributed in parallel using slab or pencil decomposition as shown in Fig. 3.

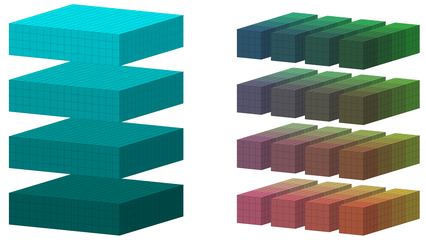

Figure 3: Slab and pencil decomposition for parallel distribution of the domain.

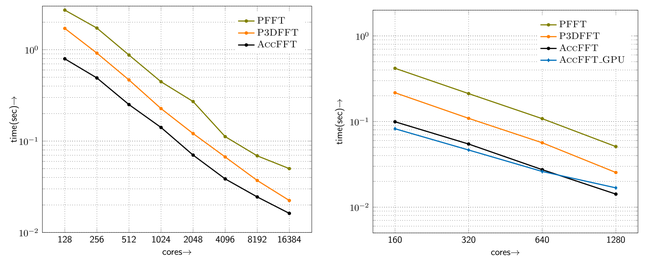

Figure 4: Strong scaling of AccFFT on Stampede (left, for $N = 1024^3$) and Maverick (right, for $N = 256 \times 512 \times 1024$) systems at TACC [1]. Wall clock time is given for a distributed 3D FFT for different GPU/core counts.

Hessian Formulation

The first order optimality conditions for eqs. (1) to (3) is as follows:

$$q(c, \alpha, p, k_f) = \begin{cases} -\frac{\partial \alpha}{\partial t} - \nabla \cdot (k\nabla\alpha) - \rho(1-2c)\alpha \\ \alpha_T + O^T\left(Oc_1 - c^*\right) \\ \frac{\partial c}{\partial t} - \nabla \cdot (k\nabla c) - \rho c(1-c) \\ c_0 - \Phi u \\ \beta_p p - \Phi^T \alpha_0 + O_0^T(O_0 \Phi p - d_0) = 0 \\ \int_0^1 \int_\Omega (k\nabla c) \cdot (\nabla\alpha) d\Omega dt = 0 \end{cases} \quad (5)$$

The corresponding second order conditions lead to the Hessian equation (see [2] for definitions):

$$\begin{bmatrix} N & 0 & J^T & Z^T \\ 0 & B_p & -\Phi^T & 0 \\ J & -\Phi & 0 & W^T \\ Z & 0 & W & 0 \end{bmatrix}_{(c^0,\alpha^0,p^0,k_f^0)} \begin{bmatrix} \tilde{c} \\ \tilde{p} \\ \tilde{\alpha} \\ \tilde{k_f} \end{bmatrix} = \begin{bmatrix} 0 \\ -g_p \\ 0 \\ -g_k \end{bmatrix}_{(c^0,\alpha^0,p^0,k_f^0)} \quad (6)$$

To solve this linear system, we use a reduced space formulation, by eliminating $\tilde{c}$ and $\tilde{\alpha}$ from the system. As a result we obtain:

$$\begin{bmatrix} H_{pp} & H_{pk} \\ H_{kp} & H_{kk} \end{bmatrix} \begin{bmatrix} \tilde{p} \\ \tilde{k_f} \end{bmatrix} = \begin{bmatrix} -g_p \\ -g_k \end{bmatrix}_{(c^0,\alpha^0,p^0,k_f^0)}, \quad (7)$$

$$(H_{pp} - H_{pk}H_{kk}^{-1}H_{kp})\tilde{p} = H_{pk}H_{kk}^{-1}g_k - g_p. \quad (8)$$

$$\tilde{k_f} = -H_{kk}^{-1}H_{kp}\tilde{p} - H_{kk}^{-1}g_k. \quad (9)$$

Results

To test the algorithm, synthetic data is created with a known distribution and diffusion coefficient. Noisy, partial observations of this data at two time points drive the inverse problem to reconstruct the inversion parameters. A sample reconstruction is shown in Fig. 5.

We have developed novel Hessian preconditioners to reduce the computational cost of the Newton method. These include two Analytical Preconditioners (AP), where we use approximate analytical solutions to the Hessian. The other approach is to use a Coarse Grid Preconditioner, where the numerical inverse of the Hessian is computed on a coarse grid. The performance of these preconditioners are shown in Tab. 1. The effectiveness of these preconditioners has led us to alter the Inexact Newton method to a Hybrid one. There we use the preconditioner instead of the numerical Hessian when the solution is far from the optimal point. This can provide considerable speedup over the Inexact Newton method as shown Tab. 2, Fig. 6.

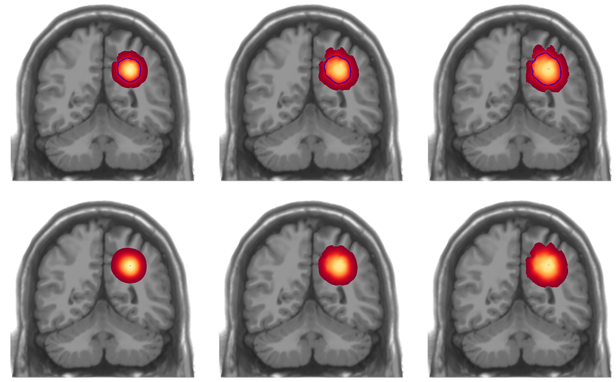

Figure 5: Target tumor distribution is shown in the top row, and the corresponding reconstructions in the bottom row. The three columns show the tumor distribution at 0, 14, and 28 months, respectively. The blue contour indicates an observable tumor concentration of $c_d = 0.2$. The reconstruction relative errors are 6.6%, 4.5% and 5.3%, respectively [2].

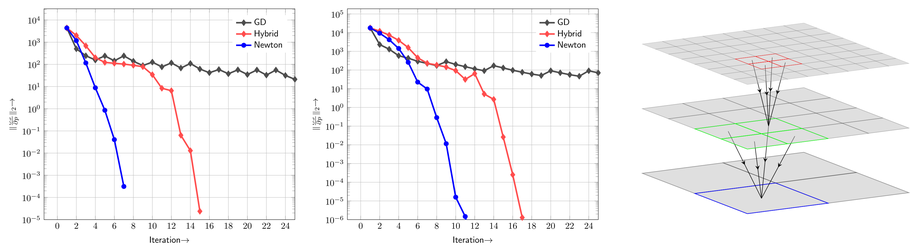

Figure 6: Convergence plot for Gradient Descent (GD), Hybrid Inexact Newton, and Inexact Newton method for $\rho = 1, 2$. Considerable speedup is achieved with the hybrid method, as shown in Table 2. Right: Illustration of the coarsening used in the Coarse Grid Preconditioner.

Table 1: The number of Hessian matvecs to solve the optimality conditions for one iteration (tol=1E-3). AP: Analytical Preconditioner, CGP_i Coarse Grid Preconditioner (level i coarsening).

ρ	No Prec	AP_0	AP_1	CGP_1	CGP_2
1.0	**7**	**3.00**	3+0.05	3+0.25	3+0.02
2.0	**8**	5.00	**3+0.05**	5+0.63	6+0.10
4.0	**9**	10.00	**3+0.06**	12+0.06	12+0.24

Table 2: Total number of Hessian matvecs necessary to reach convergence (i.e. $\|\frac{\partial J}{\partial p}\|_2 < 1\text{E-}3$) is given for different values of ρ. Significant speedup is achieved with the Hybrid Inexact Newton method.

Method	$\rho = 1.0$	$\rho = 2.0$	$\rho = 4.0$
UnPrec. Inexact Newton	**69**	**74**	**137**
Prec. Inexact Newton	34.34	38.42	47.66
Hybrid Inexact Newton	**28.06**	**28.01**	**42.6**

References

[1] Gholami, Amir, Judith Hill, Dhairya Malhotra, and George Biros. *Acc*FFT: A library for distributed-memory 3-D FFT on CPU and GPU architectures. (2015).

[2] Gholami, Amir, Andreas Mang, and George Biros. *An* inverse problem formulation for parameter estimation of a reaction-diffusion model of low grade gliomas. Journal of mathematical biology (2015): 1-25.